The Formation of Cubic *Pm*$\bar{3}$*n* Mesostructure by an Epitaxial Phase Transformation from Hexagonal *p6mm* Mesophase

Shunai Che,[†] Satoshi Kamiya,[‡] Osamu Terasaki,[‡] and Takashi Tatsumi*,[†]

Division of Materials Science and Chemical Engineering Faculty of Engineering, Yokohama National University 79-5 Tokiwadai, Yokohama 240-8501, Japan Department of Physics, Graduate School of Science Tohoku University, Sendai, 980-8578, Japan

Received July 27, 2001

Recently a variety of mesoporous materials have attracted a great deal of attention because of their controllable structures and compositions, which make them suitable for wide applications in catalysis, environmental cleanup, and advanced materials design.[1−4] The understanding of the mechanism relating to surfactant-templated reaction should ultimately lead to a more rational approach to the synthesis of mesoporous materials. There have been a number of models proposed to explain the formation of mesoporous materials and to provide a rational basis for various synthesis routes; for example, some publications have reported that MCM-48 or lamellar mesoporous materials were synthesized via the phase transformation from MCM-41, [4,5−9] and that the lamellar mesophase was transformed to MCM-48[6] or MCM-41[10] mesophases. Relatively few verification methods and experimental results, however, are available for explaining the mechanism of the synthesis of mesoporous meaterials.

We have already solved the three-dimensional structure of SBA-1 with a space group of *Pm*$\bar{3}$*n* by electron crystallography[3a,b] and reported that high-quality cubic *Pm*$\bar{3}$*n* mesoporous materials showed a highly isotropic morphology having 54 or more crystal faces.[11] Here we report that the initially generated mesophase is not cubic and that transformation of the once-formed hexagonal mesophase into the cubic phase occurs; the rate of transformation is greatly affected by the structure of trimethylbenzene (TMB) isomers and their content. The scanning electron microscope (SEM) and high-resolution transmission electron microscope (HRTEM) images observation presented visible evidence for the mesostructural constructions, indicating an epitaxial transformation from hexagonal *p6mm* to cubic *Pm*$\bar{3}$*n* mesophase.

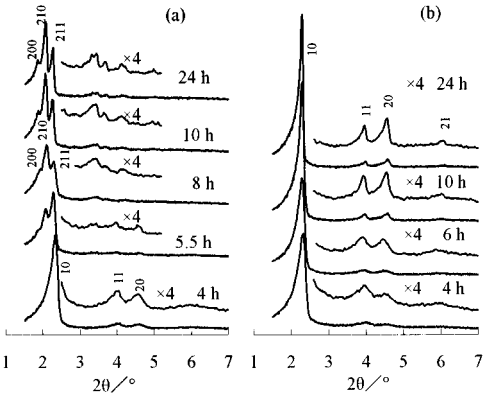

Figure 1. XRD patterns of as-synthesized materials synthesized with 1,2,3-TMB addition at 0 °C for various times. Synthesis molar composition: 1:0.13:5:125:*x* TEOS:CTEABr:HCl:H_2O: 1,2,3-TMB. 1,2,3-TMB/CTEABr = (a) 0.3 and (b) 0.5.

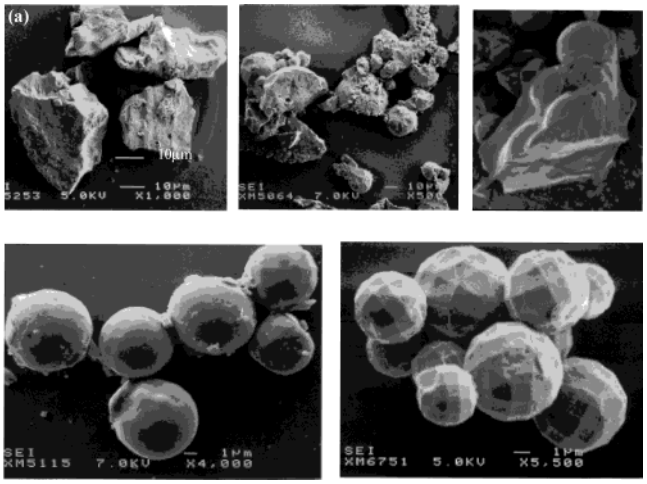

Figure 2. SEM images of the samples shown in Figure 1a. (a) 4 h, (b_1) and (b_2) 5.5 h, (c) 10 h and (d) 24 h.

Mesoporous molecular sieves were synthesized using cetyltriethylammonium bromide (CTEABr) as the surfactant, tetraethyl orthosilicate (TEOS) as a silica source and TMBs (1,3,5-TMB, 1,2,4-TMB, and 1,2,3-TMB) as cosolvent (COS). The molar composition of the reaction mixture was 0.13:1:2.5:125:*x* CTEABr:TEOS:HCl:H_2O:COS, where *x* was varied in the range of 0−0.39. The mixture was allowed to react at 0 °C under static conditions for desired times. The resultant white precipitates were filtered and dried at 100 °C overnight.

X-ray diffraction (XRD) patterns of as-synthesized materials produced with 1,2,3-TMB/CTEABr = 0.3 and 0.5 (molar ratio) are shown in Figure 1, a and b, respectively. XRD patterns were recorded using an MX Labo powder diffractometer equipped with Cu Kα radiation (40 kV, 20 mA) at the rate of 1.0° min^{-1} over the range of $2\theta = 1.5-10.0°$. The mesophases originating from the same initial mixture were sampled at different reaction times between 1 and 24 h. The materials synthesized for 4 h with 1,2,3-TMB/CTEABr = 0.3 (Figure 1a) showed the three peaks 10, 11, and 20, based on the hexagonal system, and when the synthesis was conducted to 5.5−6.5 h, three peaks in the range of $2\theta =$

* To whom correspondence should be addressed. Telephone: (81)45-339-3943. Fax: (81)45-339-3943. E-mail: ttatsumi@cms.ynu.ac.jp.
[†] Division of Materials Science & Chemical Engineering, Faculty of Engineering, Yokohama National University.
[‡] Department of Physics, Graduate School of Science and CREST, JST, Tohoku University.

(1) (a) Yanagisawa, T.; Shimizu, T.; Kuroda K.; Kato, D. *Bull. Chem. Soc. Jpn.* **1990**, *63*, 988. (b) Beck, J. S.; Vartuli, J. C.; Roth, W. J.; Leonowicz, M. E.; Kresge, C. T.; Schmitt, K. D.; Chu, C. T.-W.; Olson, D. H.; Sheppard, E. W.; McCullen, S. B.; Higgins, J. B.; Schlenker, J. L. *J. Chem. Soc.* **1992**, *114*, 10834.
(2) Monnier, A.; Schüth, F.; Huo, Q.; Kumar, D.; Margolese, D. I.; Maxwell, R. S.; Stucky, G. D.; Krishnamurty, M.; Petroff, P.; Firouzi, A.; Janicke, M.; Chmelka, B. F. *Science* **1993**, *261*, 1299.
(3) (a) Sakamoto, Y.; Kaneda, M.; Terasaki, O.; Zhao, D.; Kim, J. M.; Stucky, G. D.; Shin, H. J.; Ryoo, R. *Nature* **2000**, *408*, 449. (b) A. Carlsson, M.; Kaneda, Y.; Sakamoto, O.; Terasaki, R.; Ryoo, H.; Joo, J. *Electron Microsc.* **1999**, *48*, 795.
(4) (a) Huo, Q.; Margolese, D. I., Stucky, G. D. *Chem. Mater.* **1996**, *8*, 1147. (b) Huo, Q.; Margolese, D. I.; Ciesla, U., Demuth, D. G., Feng, P.; Gier, T. E.; Sieger, P.; Firouzi, A.; Chmelka, B. F.; Schüth, F.; Stucky, G. D. *Chem. Mater.* **1994**, *6*, 1176.
(5) Xu, J.; Luan, Z.; He, H.; Zhou, W.; Kevan, L. *Chem. Mater.* **1998**, *10*, 3690.
(6) (a) Gallis, W. K.; Landry, C. C. *Chem. Mater.* **1997**, *9*, 2035. (b) Landry, C. C.; Tolbert, S. H.; Gallis, K. W.; Monnier, A.; Stucky, G. D.; Norby, P.; Hanson, J. C. *Chem. Mater.* **2001**, *13*, 1600.
(7) Cheng, C. F.; Park, D. H.; Klinowski, J. *J. Chem. Soc., Faraday Trans.* **1997**, *93*, 193.
(8) Anderson, M. T.; Martin, J. E.; Odinek, J. G.; Newcomer, P. P. *Chem. Mater.* **1998**, *10*, 311.
(9) Adam, A. F.; Ruiz, E. J.; Tolbert, S. H. *J. Phys. Chem. B* **2000**, *104*, 5448.
(10) Matijasic, A.; Voegtlin, A. C.; Patarin, J.; Guth, J. L.; Huve, L. *Chem. Commun.* **1996**, 1123.
(11) Che, S. A.; Sakamoto, Y.; Terasaki, O.; Tatsumi, T. *Chem. Mater.* **2001**, *13*, 2237.

10.1021/ja0118237 CCC: $20.00
Published on Web 11/08/2001

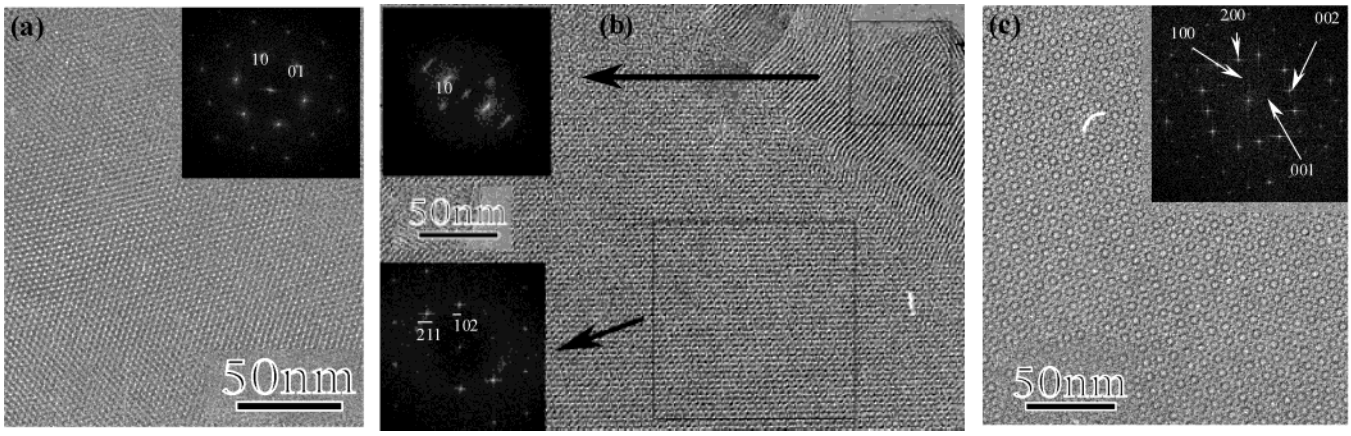

Figure 3. HREM images of the samples shown in Figure 2. (a) 4 h, (b) 5.5 h, (c) 10 h.

1.5−3.5° started to appear at the expense of the hexagonal phase peaks, which cannot be indexed to any mesophase, however. It might be estimated that these samples consisted of two types of mesophases. The three peaks of the samples obtained after 8−24 h were indexed to a set of cubic phase peaks 200, 210, and 211, indicating that the hexagonal mesophase was formed at first, and converted to the cubic $Pm\bar{3}n$ mesophase through the intermediate mixture state. As will be discussed later, the products sampled at 4 h and during 8−24 h were confirmed by EM observations to show *p6mm* and $Pm\bar{3}n$ phases, respectively. It is interesting to note that the 10 reflection of hexagonal mesophase appears to transform into the 211 reflection of cubic mesophase, which suggests a geometric correlation between the (10) planes of hexagonal phase and the (211) planes of the cubic mesophase, which was confirmed by HRTEM images later. In contrast, the hexagonal mesophase was not transformed to the cubic mesophase even after 4 days for the synthesis with 1,2,3-TMB/CTEABr = 0.5 added.

The phase transformation also occurred without any cosolvent; in the early stage the hexagonal phase was formed, but very rapidly the cubic phase evolved. The phase transformation rate was slowed with addition of TMBs, whose isomeric structure affected the rate of transformation. The hexagonal mesophase was transformed to the cubic mesophase even with 1,3,5-TMB/CTEABr = 4 added, and 1,2,4-TMB gave an intermediate effect on the phase transformation, indicating that the effects of stabilizing the hexagonal *p6mm* phase were decreased in the following order: 1,2,3-TMB > 1,2,4-TMB > 1,3,5-TMB.

The driving force for this transformation seems to be polymerization of the silica species during the synthesis. Silica condensation causes the positive charge density of the silicate network to decrease.[4a,5−10] To maintain charge matching in the interface, the organic surfactants pack to form a high surface curvature so that the transformation to the $Pm\bar{3}n$ cubic phase occurs. Apolar compound 1,3,5-TMB tends to be associated with the hydrophobic part of the surfactant micelle. The penetration of the cosolvent molecules increases the hydrophobic volume, favoring the *p6mm* phase with the low surface curvature and retarding the transformation. Asymmetrically substituted 1,2,3-TMB can enter the hydrophobic−hydrophilic "palisade" region of the micelle, resulting in a relatively large increase in the volume of the hydrophobic core to form surfactant molecule aggregates with a lower curvature surface.[4a] For the 1,2,3-TMB/CTEABr = 0.5 system, the driving force of silica polymerization might not be sufficient to increase the curvature to cause the phase transformation.

The phase transformation in the synthesis with 1,2,3-TMB/CTEABr = 0.3 can be observed clearly from SEM (Figure 2) and HRTEM images (Figure 3). It was confirmed by EM observations that the material sampled at 4 h was two-dimensional (2d) hexagonal, and the HREM image exhibited a uniform hexagonal arrangement of bright dots corresponding to the straight channels (Figure 3a).

It can be seen that the product sampled at 10 h consisted almost entirely of spherical particles (Figure 2c), which grew into crystal with 54 and 74 faces gradually when the synthesis was conducted up to 24 h (Figure 2d). We have already reported that the cubic phase having 54 crystal faces exhibits perfect HRTEM images characteristic of cubic $Pm\bar{3}n$ space group.[11] The HRTEM image (Figure 3c) for ⟨010⟩ incidence revealed regular periodicity over very large areas, and this clearly indicated that the particle is a single crystal with a well-ordered mesostructure. The material sampled at 10 h with spherical shapes proved to consist of perfect single crystals of $Pm\bar{3}n$ space group as in the case of the particles having 54 and 74 crystal faces.[11]

The sample synthesized for 5.5 h comprised particles with two types of dominant morphologies as shown in Figure 2, b_1 and b_2. One of these had the form of spheres that were observed in the sample synthesized for 10 h (Figure 2c), and the other exhibited the morphology of larger, irregular monoliths observed for the sample synthesized for 4 h (Figure 2a). It was estimated that the spheres and the monoliths corresponded to cubic and hexagonal mesophase, respectively. It can be even observed that the spherical shapes started to emerge on some monolith particles. These particular morphologies suggest that the one type of crystalline mesophases grew up on the other. The corresponding HRTEM image (Figure 3b) also showed two types of distinct mesophase patterns. The one was the typical hexagonal *p6mm* array of (10) plane, which was confirmed by tilting the specimen, and the other was the $Pm\bar{3}n$ cubic arrangement of {211} plane. These corresponded to irregular and spherical parts of the particles observed in Figure $2b_2$, respectively. Theses findings suggest that the {211} plane of cubic phase was formed via the topological changes involving silica restructuring along the cylinder axis of hexagonal phase. XRD patterns, SEM images, and HRTEM images showed that phase transformation proceeded with time from 2d-hexagonal to 3d-cubic $Pm\bar{3}n$ phase through epitaxial growth of the cubic mesophase on the hexagonal mesophase.

Acknowledgment. We are grateful to Y. Shimada (Instrumental Analysis Center, Yokohama National University,) for taking scanning electron micrographs. For financial support, O.T. thanks CREST and JST, and T.T. thanks JCII and NEDO.

JA0118237